Sampled-Data Modeling and Analysis of One-Cycle Control and Charge Control

Chung-Chieh Fang, *Member, IEEE*

***Abstract*—Sampled-data modeling and analysis are applied to PWM dc–dc converters under one-cycle control or its special case, charge control. These two control schemes are analyzed in a unified framework. Large-signal analysis, steady-state analysis and small-signal analysis are addressed analytically. The orbital nature of the nominal periodic solution is preserved. Various transfer functions are derived. Compared with the averaging approach, the sampled-data approach is more accurate and systematic.**

***Index Terms*—Charge control, dc–dc converter, one-cycle control, orbital stability, sampled-data modeling.**

I. Introduction

SAMPLED-DATA modeling and analysis are applied to PWM dc–dc converters under one-cycle control or its special case, charge control. These two control schemes are analyzed in a unified framework. Large-signal analysis, steady-state analysis and small-signal analysis are addressed analytically. The orbital nature of the nominal periodic solution is preserved. Various transfer functions are derived. They are control-to-output voltage transfer function, control-to-inductor current transfer function, audio-susceptibility, and output impedance.

One-cycle control [1]–[3] and charge control [4]–[8] have been analyzed using the averaging approach. In the averaging approach, each circuit module is modeled *separately* and *approximately*. For example, the switches are approximated as a three-terminal model. The current loop is obtained using sampled-data dynamics and then approximated by continuous-time dynamics. The duty cycle, a *discrete-time* variable, is treated as a continuous-time variable. Then all of these approximate modules form a continuous-time model. Therefore, the *orbital* nature of the nominal periodic solution is lost. Instead, an equilibrium is obtained as the nominal solution.

In contrast, no such approximations are involved in the sampled-data approach. The orbital nature of the nominal periodic solution is preserved. Also, the sampled-data approach focuses on the *system* operations, especially the *switching* action. The switching action is very important for the derivation of system dynamics. Once the switching action is accurately formulated, the large-signal and small-signal sampled-data dynamics can be easily obtained. Therefore, the advantage of the sampled-data approach is that it is more accurate and systematic. Although sampled-data analysis of converters has been a topic of investigation for the past two decades [9]–[15], this powerful tool is not widely used. This paper has an aim to increase the appreciation and use of the sampled-data approach.

Manuscript received May 27, 1999; revised January 5, 2001. Recommended by Associate Editor K. Smedley.

The author is with the Logic Library Department, Taiwan Semiconductor Manufacturing Company, Hsinchu, Taiwan 300, R.O.C. (e-mail: chungchiehfang@yahoo.com).

Publisher Item Identifier S 0885-8993(01)04030-3.

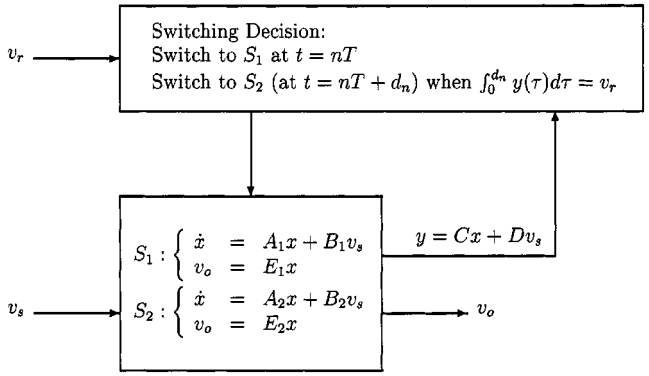

Fig. 1. Block diagram model for one-cycle control or charge control.

In this paper, the operation of continuous conduction mode with constant switching frequency is considered. Other operations, like discontinuous conduction mode or variable switching frequency, can be modeled and analyzed similarly.

The remainder of the paper is organized as follows. In Section II, a block diagram model is proposed for the PWM dc–dc converter under one-cycle control or its special case, charge control. In Sections III–VI, large-signal, steady-state, small-signal and stability analysis are addressed. In Sections VII and VIII, various transfer functions are derived. In Section IX, two illustrative examples are given. Conclusions are collected in Section X.

II. Exact Block Diagram Model

The operation of one-cycle control (or its special case, charge control) can be described in terms of the block diagram model shown in Fig. 1. The model is so general that it can be applied to most PWM converters, such as buck, boost, buck–boost, and Ćuk converters. In the diagram model, A_1, $A_2 \in \mathbf{R}^{N\times N}$, B_1, $B_2 \in \mathbf{R}^{N\times 1}$, C, E_1, $E_2 \in \mathbf{R}^{1\times N}$, and $D \in \mathbf{R}$ are constant matrices, where N is the state dimension, typically given by the number of energy storage elements in the power stage. For example, $N = 2$ for a typical buck converter and $N = 4$ for a Ćuk converter. Also in the diagram, v_s is the source voltage, v_o is the output voltage, $x \in \mathbf{R}^N$ is the state, $y = Cx + Dv_s \in \mathbf{R}$ is a combination of state feedback Cx and feedforward from v_s, and v_r is a reference signal, which controls switching actions as described next.

Let the switching period be T, which is inverse of the switching frequency f_s. Within the cycle $t \in [nT, (n+1)T)$, the dynamics is switched between two stages, S_1 and S_2. Each stage has linear dynamics as shown in the diagram. The system is in S_1 at the beginning of the cycle, and switches to S_2 at $t = nT + d_n$ when $\int_0^{d_n} y(\tau)\,d\tau = v_r$. In this control scheme, the duty cycle $D_c = d_n/T$ is controlled by the integration value of the signal y.

The two matrices E_1 and E_2 need not be the same. For example, they can differ if the equivalent series resistance (ESR) $R_c \neq 0$. When they differ, the output voltage is discontinuous. Let E denote E_1, E_2 or $(E_1+E_2)/2$, depending on which sampled output voltage is of interest.

Since the block diagram model in Fig. 1 *exactly* describes the operation of one-cycle control or its special case, charge control, the sampled-data dynamics derived from this model is expected to be accurate. The derivation is discussed in the following sections.

III. Nonlinear Large-Signal Dynamics

Consider the cycle $t \in [nT, (n+1)T)$. Let the sampled signals $x_n = x(nT)$ and $v_{on} = v_o(nT)$. Generally in the PWM dc–dc converter, the switching frequency is sufficiently high that the variations in v_s and v_r within the cycle are small and can be neglected. Take v_s and v_r to be constant within the cycle and denote them as v_{sn} and v_{rn}, respectively. The notation v_{sn} instead of $v_{s,n}$ is used for brevity. This notation applies to other variables.

From the operation in Fig. 1, the large-signal sampled-data dynamics of the power stage is

$$\begin{aligned} x_{n+1} &= f(x_n, v_{sn}, d_n) \\ &= e^{A_2(T-d_n)} \cdot \left(e^{A_1 d_n} x_n + \int_0^{d_n} e^{A_1\sigma}\,d\sigma B_1 v_{sn} \right) \\ &\quad + \int_0^{T-d_n} e^{A_2\sigma}\,d\sigma B_2 v_{sn} \\ v_{\rm on} &= E x_n \end{aligned}$$

$$\begin{aligned} g(x_n, v_{sn}, d_n, v_{rn}) &= \int_0^{d_n} y(\tau)\,d\tau - v_{rn} \\ &= C \int_0^{d_n} \cdot \left(e^{A_1\tau} x_n + \int_0^{\tau} e^{A_1\sigma}\,d\sigma B_1 v_{sn} \right) d\tau \\ &\quad + D v_{sn} d_n - v_{rn} = 0. \end{aligned} \tag{1}$$

It is a closed-loop dynamics: a power stage $x_{n+1} = f(x_n, v_{sn}, d_n)$ with a feedback loop determined by $g(x_n, v_{sn}, d_n, v_{rn}) = 0$. It is also a constrained nonlinear discrete-time dynamics. The constraint equation $g(x_n, v_{sn}, d_n, v_{rn}) = 0$ determines the switching instant d_n. The dynamics is derived *directly* from the switching operation in Fig. 1. This approach is more accurate than the averaging approach, where the dynamics of each circuit module is approximated *separately*.

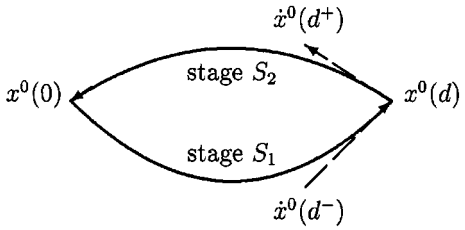

Fig. 2. Typical periodic solution $x^0(t)$ in state space.

IV. Steady-State Analysis: Finding a Periodic Solution

The nominal solution of a dc–dc converter is a *periodic orbit*, not an equilibrium point as depicted in the averaging approach. Let the nominal (set-point) output voltage be $V_{\rm SET}$. A periodic orbit $x^0(t)$ in Fig. 1 corresponds to a fixed point $x^0(0)$ in the sampled-data dynamics (1). Let the fixed point be $(x_n, v_{sn}, d_n, v_{rn}) = (x^0(0), V_s, d, V_r)$, where d/T is the steady-state duty cycle. Then this fixed point satisfies

$$\begin{aligned} x^0(0) &= f\left(x^0(0), V_s, d\right) \\ E x^0(0) &= V_{\rm SET} \\ g\left(x^0(0), V_s, d, V_r\right) &= 0. \end{aligned} \tag{2}$$

From (2), one sees that the feedback loop, denoted by the constraint equation, affects the fixed point. The $N+2$ nonlinear equations [see (2)] in $N+2$ unknowns [$x^0(0)$, d and V_r] can be solved by Newton's method. After obtaining the steady-state values $x^0(0)$, d and V_r, a periodic solution $x^0(t)$ is obtained

$$x^0(t) = \begin{cases} e^{A_1 t} x^0(0) \\ \quad + \displaystyle\int_0^t e^{A_1(t-\sigma)}\,d\sigma B_1 V_s, & \text{for } t \in [0,\, d) \\ e^{A_2(t-d)} x^0(d) \\ \quad + \displaystyle\int_d^t e^{A_2(t-\sigma)}\,d\sigma B_2 V_s, & \text{for } t \in [d,\, T) \\ x^0(t \bmod T), & \text{for } t \geq T. \end{cases} \tag{3}$$

A typical periodic solution $x^0(t)$ is shown Fig. 2. In the figure, the dashed arrows denote the time derivative of $x^0(t)$ at $t = d^-$ and d^+ [which are $\dot{x}^0(d^-) = A_1 x^0(d) + B_1 V_s$ and $\dot{x}^0(d^+) = A_2 x^0(d) + B_2 V_s$ respectively]. These abbreviated notations are used in the next section to simplify the linearized dynamics.

V. Analytical Small-Signal Dynamics

Assume a fixed point $(x_n, v_{sn}, d_n, v_{rn}) = (x^0(0), V_s, d, V_r)$ exists. Use the notation $\diamondsuit$ to denote evaluation at this fixed point and use a hat $\hat{}$ to denote small perturbations [e.g., $\hat{x}_n = x_n - x^0(0)$]. The system (1) has the linearized (small-signal) dynamics

$$\begin{aligned} \hat{x}_{n+1} &\approx \Phi \hat{x}_n + \Gamma_v \hat{v}_{sn} + \Gamma_r \hat{v}_{rn} \\ \hat{v}_{on} &= E \hat{x}_n \end{aligned} \tag{4}$$

where $\Phi \in \mathbf{R}^{N\times N}$ and Γ_s, $\Gamma_r \in \mathbf{R}^{N\times 1}$ are as follows:

$$\Phi = \left.\frac{\partial f}{\partial x_n} - \frac{\partial f}{\partial d_n}\left(\frac{\partial g}{\partial d_n}\right)^{-1}\frac{\partial g}{\partial x_n}\right|_{\diamond}$$

$$\Gamma_v = \left.\frac{\partial f}{\partial v_{sn}} - \frac{\partial f}{\partial d_n}\left(\frac{\partial g}{\partial d_n}\right)^{-1}\frac{\partial g}{\partial v_{sn}}\right|_{\diamond}$$

$$\Gamma_r = \left.-\frac{\partial f}{\partial d_n}\left(\frac{\partial g}{\partial d_n}\right)^{-1}\frac{\partial g}{\partial v_{rn}}\right|_{\diamond}$$

$$\left.\frac{\partial f}{\partial x_n}\right|_{\diamond} = e^{A_2(T-d)}e^{A_1 d}$$

$$\left.\frac{\partial f}{\partial d_n}\right|_{\diamond} = e^{A_2(T-d)}\left(\dot{x}^0(d^-) - \dot{x}^0(d^+)\right)$$

$$\left.\frac{\partial g}{\partial d_n}\right|_{\diamond} = Cx^0(d) + DV_s = y^0(d)$$

$$\left.\frac{\partial g}{\partial x_n}\right|_{\diamond} = C\int_0^d e^{A_1\tau}\,d\tau$$

$$\left.\frac{\partial f}{\partial v_{sn}}\right|_{\diamond} = e^{A_2(T-d)}\int_0^d e^{A_1\sigma}\,d\sigma B_1 + \int_0^{T-d} e^{A_2\sigma}\,d\sigma B_2$$

$$\left.\frac{\partial g}{\partial v_{sn}}\right|_{\diamond} = C\int_0^d\int_0^\tau e^{A_1\sigma}\,d\sigma\,d\tau B_1 + Dd$$

$$\left.\frac{\partial g}{\partial v_{rn}}\right|_{\diamond} = -1.$$

Therefore

$$\Phi = e^{A_2(T-d)} \cdot \left(e^{A_1 d} - \left(\dot{x}^0(d^-) - \dot{x}^0(d^+)\right)C\int_0^d e^{A_1\tau}\,d\tau / y^0(d)\right) \tag{5}$$

$$\Gamma_v = e^{A_2(T-d)}\int_0^d e^{A_1\sigma}\,d\sigma B_1 + \int_0^{T-d} e^{A_2\sigma}\,d\sigma B_2 - e^{A_2(T-d)}\left(\dot{x}^0(d^-) - \dot{x}^0(d^+)\right) \cdot \left(C\int_0^d\int_0^\tau e^{A_1\sigma}\,d\sigma\,d\tau B_1 + Dd\right)\Big/ y^0(d) \tag{6}$$

$$\Gamma_r = e^{A_2(T-d)}\left(\dot{x}^0(d^-) - \dot{x}^0(d^+)\right)/y^0(d). \tag{7}$$

Once the fixed point $(x^0(0),\, V_s,\, d,\, V_r)$ is obtained as in Section IV, the matrices Φ, Γ_v and Γ_r are readily obtained from (5)–(7).

The small-signal dynamics (4) is obtained *directly* and *exactly* from the linearization of the large-signal dynamics (1). This approach is more systematic and accurate than the averaging approach, where the small-signal dynamics is sometimes obtained *approximately* from graphical analysis.

VI. Orbital Stability and Stabilizability

The relevant stability notion is asymptotic *orbital* stability, not asymptotic stability of an equilibrium point as depicted in the averaging approach. In the power electronics literature, the PWM dc–dc converter is generally said to be either stable or unstable, without mentioning orbital stability *per se*. The definition of asymptotic orbital stability is given as follows.

Definition 1 (see, e.g., [16]): Denote by γ the closed orbit generated by the periodic solution $x^0(t)$. Then $x^0(t)$ is asymptotically orbitally stable if there is a δ such that

$$\text{dist}\,[x(0),\,\gamma] < \delta \Rightarrow \lim_{t\to\infty}\text{dist}\,[x(t),\,\gamma] = 0$$

where dist$[z,\,\gamma]$ is defined as the smallest distance between the point z and any point on γ.

The orbital stability is related to the set of eigenvalues of Φ. The periodic solution $x^0(t)$ is asymptotically orbitally stable if all of the eigenvalues of Φ are inside the unit circle of the complex plane [16].

The reference signal v_r is used as a control variable. The question whether the power stage can be stabilized by using v_r is answered by the following theorem. The answer is yes because the stated assumption in the theorem is generally satisfied.

Theorem 1: Assume that all of the eigenvalues of at least one of A_1 and A_2 are in the open left half of the complex plane, and that neither matrix has any eigenvalue in the open right half of the complex plane. Then the system (1) or the original continuous-time system of Fig. 1 is stabilizable by using v_r.

Proof: Let $K = C\int_0^d e^{A_1\tau}\,d\tau$. Then $\Phi + \Gamma_r K = e^{A_2(T-d)}e^{A_1 d}$ has eigenvalues inside the unit circle under the stated assumption [17]. Therefore, a discrete-time control law $v_{rn} = Kx_n$ can stabilize the system (1) or the original continuous-time system of Fig. 1. □

VII. Control-to-Output Voltage and Control-to-Inductor Current Transfer Functions

From (4), the control-to-output voltage transfer function is

$$T_{oc}(z) = \frac{\hat{v}_o(z)}{\hat{v}_r(z)} = E(zI-\Phi)^{-1}\Gamma_r. \tag{8}$$

Let $E_I \in \mathbf{R}^{1\times N}$ be chosen such that $E_I x = i_L$ (inductor current). Then the control-to-inductor current transfer function is

$$T_{ic}(z) = \frac{\hat{i}_L(z)}{\hat{v}_r(z)} = E_I(zI-\Phi)^{-1}\Gamma_r. \tag{9}$$

Given a transfer function in z domain, say $T(z)$, its effective frequency response [18] is $T(e^{j\omega T})$, which is valid in the frequency range $|\omega| < \pi/T$.

VIII. Audio-Susceptibility and Output Impedance

Audio-susceptibility and output impedance are expressed in terms of transfer functions (frequency responses). They give information on the effect of (source or load) disturbances at various frequencies on the output voltage.

The audio-susceptibility is derived directly from the linearized sampled-data model, (4). It is

$$T_{os}(z) = \frac{\hat{v}_o(z)}{\hat{v}_s(z)} = E(zI - \Phi)^{-1}\Gamma_s. \tag{10}$$

To calculate the output impedance, add a fictitious current source i_o (as perturbation) in parallel with the load. Then the state equations in Fig. 1 are replaced by

$$S_1\colon \dot{x} = A_1 x + B_1 v_s + B_{i1} i_o \tag{11}$$

$$S_2\colon \dot{x} = A_2 x + B_2 v_s + B_{i2} i_o \tag{12}$$

where $B_{i1}, B_{i2} \in \mathbf{R}^{N\times 1}$.

Since i_o is used as perturbation, the nominal value of i_o is 0. Similar to the derivation in Section V, the new linearized sampled-data dynamics is

$$\begin{aligned} \hat{x}_{n+1} &\approx \Phi\hat{x}_n + \Gamma_s\hat{v}_{sn} + \Gamma_r\hat{v}_{rn} + \Gamma_i\hat{i}_{on} \\ \hat{v}_{on} &= E\hat{x}_n \end{aligned} \tag{13}$$

where i_{on} is the sampled perturbed output current and

$$\begin{aligned} \Gamma_i = &\frac{\partial f}{\partial i_{on}} - \frac{\partial f}{\partial d_n}\left(\frac{\partial g}{\partial d_n}\right)^{-1} \\ &\cdot \left.\frac{\partial g}{\partial i_{on}}\right|_{(x_n, v_{sn}, d_n, v_{rn}, i_{on})=(x^0(0), V_s, d, V_r, 0)} \\ = &e^{A_2(T-d)}\int_0^d e^{A_1\sigma}\,d\sigma B_{i1} + \int_0^{T-d} e^{A_2\sigma}\,d\sigma B_{i2} \\ &- e^{A_2(T-d)}\left(\dot{x}^0(d^-) - \dot{x}^0(d^+)\right) \\ &\cdot \left(C\int_0^d\int_0^\tau e^{A_1\sigma}\,d\sigma\,d\tau B_{i1} + Dd\right)\Big/\, y^0(d). \end{aligned} \tag{14}$$

So the output impedance is

$$T_{oo}(z) = \frac{\hat{v}_o(z)}{\hat{i}_o(z)} = E(zI - \Phi)^{-1}\Gamma_i. \tag{15}$$

IX. Illustrative Examples

Example 1 (Buck Converter Under One-Cycle Control, [1]): The power stage parameters of the buck converter are $V_s = 10$ V, switching frequency $f_s = 1/T = 30$ kHz, $L = 0.48$ mH, $C = 30$ μF (with ESR $R_c = 0$ Ω), and load $R = 25$ Ω. Let the steady-state duty cycle D_c be 0.64, then the switching instant $d = 0.64T = 2.13\times 10^{-5}$. The voltage across the diode during the ON stage S_1, which equals V_s, is integrated. Then $V_r = V_s\,d = 2.13\times 10^{-4}$.

Let the state $x = (i_L, v_C)' \in \mathbf{R}^{2\times 1}$, where i_L is the inductor current and v_C is the capacitor voltage. In terms of the block diagram model in Fig. 1, one has

$$A_1 = A_2 = \begin{bmatrix} \dfrac{-RR_c}{(R+R_c)L} & \dfrac{-R}{(R+R_c)L} \\ \dfrac{R}{(R+R_c)C} & \dfrac{-1}{(R+R_c)C} \end{bmatrix}$$

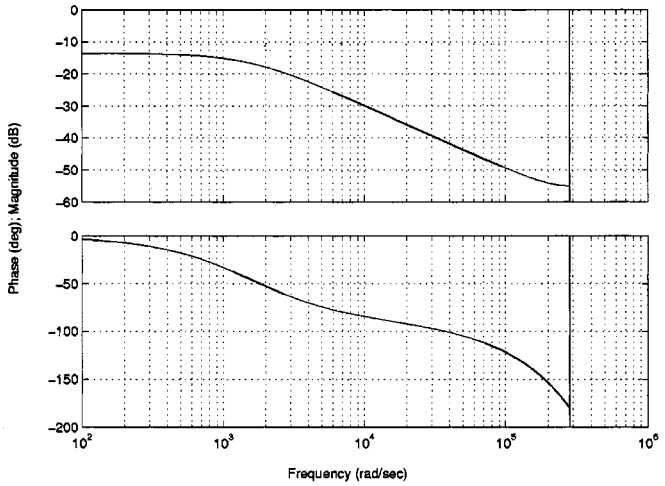

Fig. 3. Audio-susceptibility of Example 2.

$$B_1 = \begin{bmatrix} \dfrac{1}{L} \\ 0 \end{bmatrix} \qquad B_2 = \begin{bmatrix} 0 \\ 0 \end{bmatrix}$$

$$C = [0 \quad 0] \qquad D = 1$$

$$E_1 = E_2 = \left[\frac{RR_c}{R+R_c} \quad \frac{R}{R+R_c}\right].$$

From (5), the matrix $\Phi = e^{A_1 T}$ has eigenvalues at $0.94 \pm 0.267i$, which are inside the unit circle, and the system is asymptotically stable. It is reasonable because here $y = v_s$ is a feedforward without state feedback.

Example 2—(Buck Converter Under Charge Control, [4]): The power stage parameters of the buck converter are $V_s = 12$ V, switching frequency $f_s = 90$ kHz, $L = 37.5$ μH, $C = 380$ μF (with ESR $R_c = 20$ mΩ), and load $R = 3.375$ Ω. The duty cycle D_c is 0.42, then $d = 0.42T = 4.67\times 10^{-6}$. The switch current during the ON stage S_1, which equals the inductor current i_L, is integrated through a charging capacitance $C_T = 733$ nF.

Let the state $x = (i_L, v_C)'$. In terms of the block diagram model in Fig. 1, one has the same system matrices as in Example 1 except here the matrices $C = [1/C_T, 0]$ and $D = 0$. Different from Example 1, here the system has state feedback. Solving (2) gives $x^0(0) = (1.06, 5.04)'$, $x^0(d) = (1.93, 5.04)'$, and $V_r = 9.51$. The eigenvalues of Φ calculated from (5) are 0.22 and 0.98. Therefore the system is asymptotically stable.

The audio-susceptibility is shown in Fig. 3. The control-to-output voltage and control-to-inductor current transfer functions are shown in Figs. 4 and 5, respectively, and they are compared with the those of the averaged model in [4]. The magnitude responses are similar, but the phase responses are different at high frequency. From the control-to-output voltage transfer functions, the sampled-data model has gain margin 53.1 dB (452); the average model 126.2 dB (2.04×10^6).

Many approaches exist to verify the validity of power stage models. One common approach involves using a dynamic analyzer to determine which model gives a frequency response most in agreement with experimental data. Here another approach is used. Since the *exact closed-loop* stability can be determined

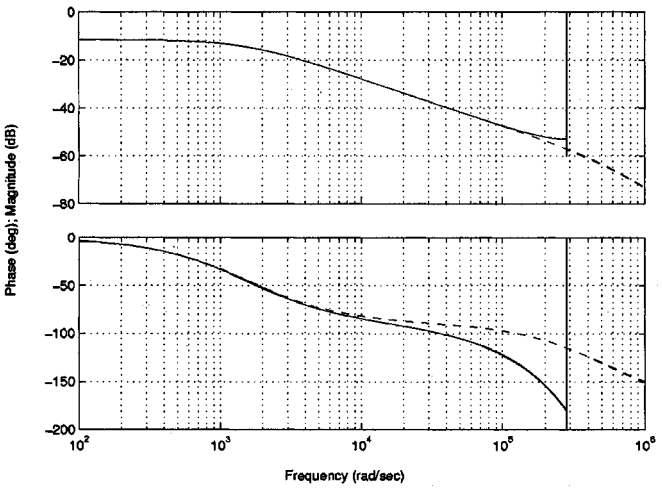

Fig. 4. Control-to-output voltage transfer function (solid line: sampled-data model; dashed line: averaged model in [4]).

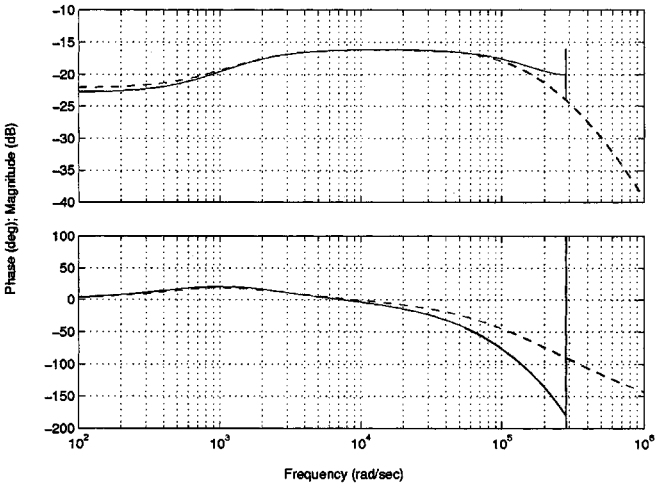

Fig. 5. Control-to-inductor current transfer function (solid line: sampled-data model; dashed line: averaged model in [4]).

as shown in [19], [20], the true gain margin can also be determined. Therefore, gain margin will be used to verify the validity of power stage models.

Generally the controller for a PWM converter uses dynamic feedback, with an integrator enclosed. For simplicity, the following static feedback is used: $v_r = g(V_R - v_o)$, where g is a feedback gain and $V_R = Ex^0(0) + V_r/g = 5.03 + 9.51/g \approx 5.03$. (To ensure the duty cycle is fixed at 0.42, V_R is varied according to g. However, it is close to 5.03.) The true gain margin, determined by *exact* closed-loop analysis [19], [20], is exactly 53.1 dB. It is the same as predicted by the sampled-data model. [For $g > 452$ (53.1 dB), one eigenvalue of Φ is less than -1, and a period-doubling bifurcation occurs.] Therefore in this example, the sampled-data model has better prediction of closed-loop instability than the averaged model in [4].

X. Conclusions

Sampled-data modeling and analysis have been applied to PWM dc–dc converters under one-cycle control or its special case, charge control. These two control schemes have been analyzed in a unified framework. Large-signal, steady-state and small-signal analysis have been addressed analytically. The orbital nature of the nominal periodic solution has been preserved. Various transfer functions have been derived.

In the sampled-data approach, the system dynamics is derived *directly* and *exactly* from discrete switching operations. For example, the switching operation of one-cycle control is exactly modeled by Fig. 1 and its sampled-dynamics is exactly (1). In the averaging approach, however, each circuit module is modeled *separately* and *approximately*. Therefore, the sampled-data approach is more systematic and accurate than the averaging approach.

The sampled-data approach is generally believed to be numerical intensive and is not widely used. However, the only numerical intensive procedure in the sampled-data approach is to find the fixed-point by solving (2). The remaining analysis is eased by the *analytical* form of the dynamic models. For example, once the fixed-point is obtained, the matrices Φ, Γ_v, and Γ_r can be obtained from (5)–(7). Then the linearized dynamics and various transfer functions are then easily obtained. The sampled-data modeling and analysis can be applied systematically to dc–dc converters under various configurations [15], including voltage mode control, current mode control, and hysteretic control. It is hoped that this work will help to facilitate further applications of the sampled-data approach in power electronics.

References

[1] K. M. Smedley and S. Ćuk, "One-cycle control of switching converters," *IEEE Trans. Power Electron.*, vol. 10, pp. 625–633, Nov. 1995.
[2] E. Santi and S. Ćuk, "Modeling of one-cycle controlled switching converters," in *Proc. INTELEC*, 1992, pp. 131–138.
[3] K. M. Smedley and S. Ćuk, "Dynamics of one-cycle controlled Ćuk converters," *IEEE Trans. Power Electron.*, vol. 10, pp. 634–639, Nov. 1995.
[4] W. Tang, F. C. Lee, R. B. Ridley, and I. Cohen, "Charge control: Modeling, analysis and design," in *Proc. IEEE PESC*, 1992, pp. 503–511.
[5] ——, "Charge control: Modeling, analysis, and design," *IEEE Trans. Power Electron.*, vol. 8, pp. 396–403, July 1993.
[6] F. A. Huliehel, W. Tang, F. C. Lee, and B. H. Cho, "Modeling, analysis, and design of the quasicharge control," *IEEE Trans. Power Electron.*, vol. 10, pp. 597–604, Sept. 1995.
[7] V. Vorperian, "The charge-controlled PWM switch," in *Proc. IEEE PESC*, 1996, pp. 533–542.
[8] J. Sun, W.-C. Wu, and R. Bass, "Large-signal characterization of single-phase PFC circuits with different types of current control," in *Proc. APEC*, 1998, pp. 655–661.
[9] F. C. Y. Lee, R. P. Iwens, Y. Yu, and J. E. Triner, "Generalized computer-aided discrete time-domain modeling and analysis of dc–dc converters," *IEEE Trans. Ind. Electron. Contr. Instrum.*, vol. IECI-26, pp. 58–69, Apr. 1979.
[10] A. R. Brown and R. D. Middlebrook, "Sampled-data modeling of switching regulators," in *Proc. IEEE PESC*, 1981, pp. 349–369.
[11] G. C. Verghese, M. Elbuluk, and J. G. Kassakian, "A general approach to sample-data modeling for power electronic circuits," *IEEE Trans. Power Electron.*, vol. 1, pp. 76–89, Mar. 1986.
[12] R. Lutz and M. Grotzbach, "Straightforward discrete modeling for power converter systems," in *Proc. IEEE PESC*, 1986, pp. 761–770.
[13] R. Tymerski, "Frequency analysis of time-interval-modulated switched networks," *IEEE Trans. Power Electron.*, vol. 6, pp. 287–295, Mar. 1991.
[14] ——, "Application of the time-varying transfer function for exact small-signal analysis," *IEEE Trans. Power Electron.*, vol. 9, pp. 196–205, Mar. 1994.
[15] C.-C. Fang, "Sampled-data analysis and control of dc–dc switching converters," Ph.D. dissertation, Univ. Maryland, College Park, MD, 1997.
[16] H. K. Khalil, *Nonlinear Systems*. New York: Macmillan, 1992.

[17] C.-C. Fang and E. H. Abed. (1998) Feedback stabilization of PWM dc–dc converters. Inst. Syst. Research, Univ. Maryland, College Park. [Online]. Available: www.isr.umd.edu/TechReports/ISR/1998.
[18] A. V. Oppenheim and R. W. Schafer, *Discrete-Time Signal Processing*. Englewood Cliffs, NJ: Prentice-Hall, 1989, p. 93.
[19] C.-C. Fang and E. H. Abed. (1998) Sampled-data modeling and analysis of PWM dc–dc converters—I. Closed-loop circuits. Inst. Syst. Research, Univ. Maryland, College Park. [Online]. Available: www.isr.umd.edu/TechReports/ISR/1998.
[20] ——, "Sampled-data modeling and analysis of closed-loop PWM dc–dc converters," in *Proc. IEEE ISCAS*, vol. 5, 1999, pp. 110–115.

Chung-Chieh Fang (M'98) received the B.S. degree from National Taiwan University (NTU), Taipei, Taiwan, R.O.C., in 1990, and the M.S. and Ph.D. degrees from the University of Maryland, College Park, in 1991 and 1997, respectively, all in electrical engineering.

He was a Product Engineer at WaferTech, Camas, WA, in 1998 and a Post-Doctor at NTU, in 1999. He is currently a Circuit Engineer at Taiwan Semiconductor Manufacturing, Co., Hsinchu. His research interests include modeling, analysis, and design of nonlinear circuits and systems.